Chapter 5. Numerical and experimental analysis for calibration of the magneto-elastic material parameters

5.1. Introduction

The nature of the failure in a giant magnetostrictive bi-nonlinear material is influenced by the state of tension and compression regions in the flexure loading. Comprehensive numerical and experimental studies on the Terfenol-D SENB specimens are required to characterize the fracture parameters of giant magnetostrictive material (GMM) (for SENB specimens) in the coupled magneto-elastic field. The giant magnetostrictive material Terfenol-D ($Tb_{0.27}Dy_{0.73}Fe_{1.93}$) is selected for this investigation and procured from Lanzhou Jian Xing Commercial and Trading Co., Ltd. in cylindrical rod and cuboid bar shapes with a diameter of 8 mm and a cross-section of $3.5 \times 3.5\ \mathrm{mm}^2$, respectively. The Terfenol-D specimens have an easy axis along its longitudinal direction. In order to employ the proposed constitutive model for numerical fracture characterization, the parameters of the giant magnetostrictive material must be determined. These parameters can be optimized using the finite element procedures and some physics-based experiments. Since, Terfenol-D magnetization and magnetostrictive characteristics are heavily sensitive to magnetic and mechanical bias conditions; hence accurate characterization of this material is required for its exploitation. Apart from this, the elastic modulus variability generates nonlinearities in the material response and that must be quantified by tensile or compression experimentations. Thus, in this chapter, the physics-based experiments are conducted for the hysteretic magnetic response characterization, specifically for the magnetization and magnetostriction loops. Compression experiments in the presence and absence of magnetic fields are preferred in this work to analyse the nonlinearity in the stress-strain curves. This is because, Terfenol-D is a highly brittle intermetallic material and very much fragile under

tensile stresses. Not only, it is arduous to prepare a specimen for direct tension testing, but also it is notorious to be reported to break at the grip itself rather than gage section during tension testing [18]. The stress-strain curve's nature of Terfenol-D under tension was adequately explained earlier in literature by Butler and Jiles [4,28] and hence therefore it is pertinent that compressive stress-strain curves are sufficient to optimize the material parameters in the present case.

5.2. Experimental characterization

In this section, the magneto-elastic coupled field experimentation for magnetization, magnetostriction, and compressive stress-strain material testing have been carried out as per the outlines described in the respective ASTM standards [128–130].

5.2.1. Hysteretic magnetic response characterization set up

Figure 5.1 shows the experimental arrangement for obtaining the hysteretic magnetic response characterization, specifically for the magnetization and magnetostriction loops. Two types of measurements are performed for the different constant pressure levels; (a) the magnetic field is modulated to produce magnetization hysteresis loops, and (b) the magnetic field is modulated to produce magnetostriction hysteresis loops. A water-cooled electromagnet (Polytronic EM-150) with 150 mm diameter pole pieces along with the bi-polar power supply (Polytronic BCS-150) is used for this purpose to generate a variable external magnetic field. The bi-polar power supply (Polytronic BCS-150) is a current stabilizing power supply capable of providing a variable current from -30 A through zero to +30 A (and vice versa) with a +/- 60 V. The bi-polar power supply has 0.05% stability at set value with constant external effects. One of its pole pieces is modified with a 40 mm diameter piston which is actuated hydraulically by a hand pump, and a bottom entry Bourdon tube pressure gauge (WIKA 7075660) is used to measure the pressure behind the piston. The

compressive stress up to 60 MPa is applied to the Terfenol-D rod sample having 8 mm diameter and 28 mm length.

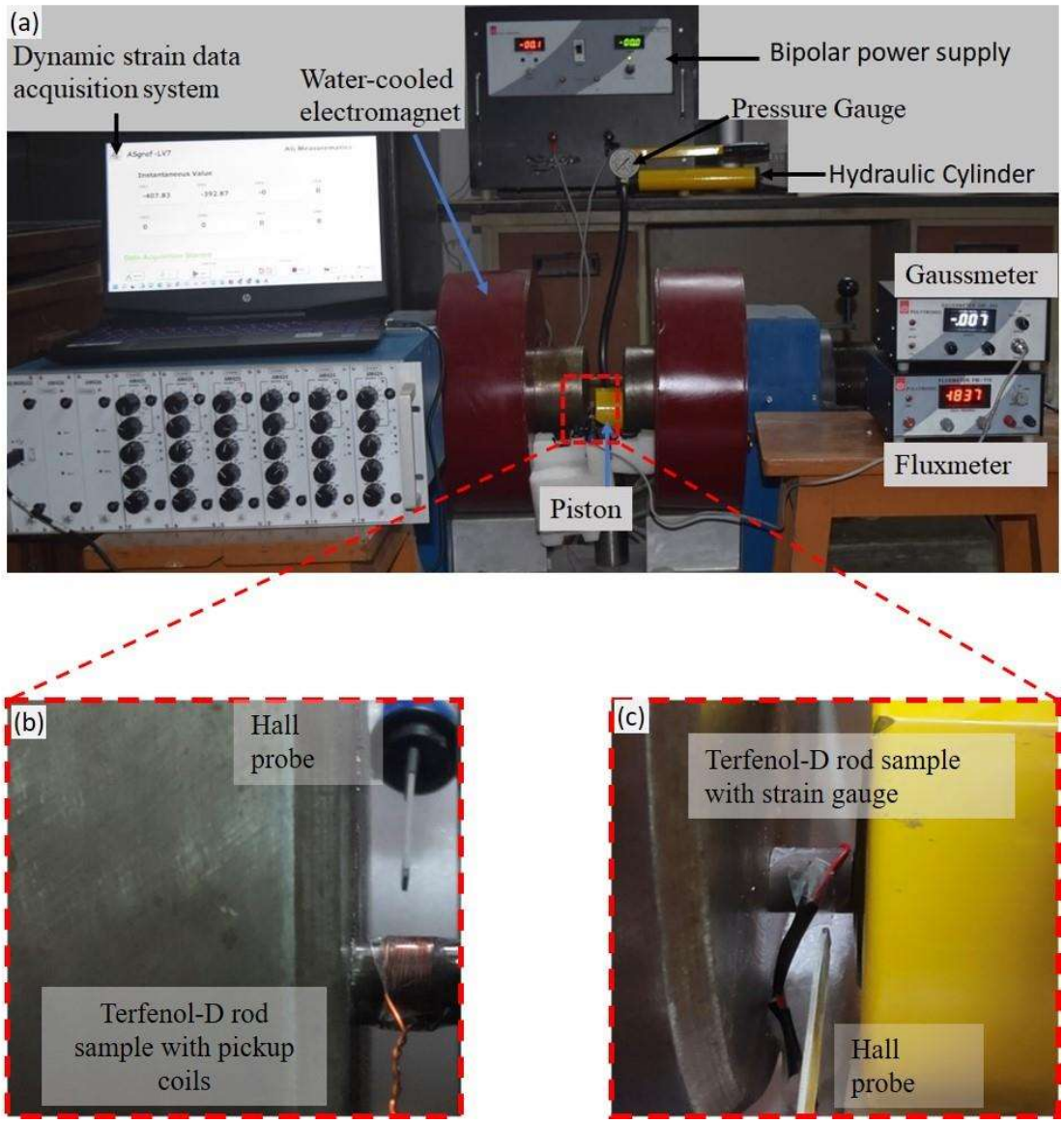

Figure 5.1 (a) Experimental arrangement for magnetization and magnetostriction test **(b)** Terfenol-D sample with pickup coils and Hall probe in a zoomed-in perspective **(c)** Terfenol-D sample with strain gauge and Hall probe in a zoomed-in perspective

The external magnetic field strength is measured using a Hall effect gaussmeter (Polytronic GM-504) probe placed near the rod sample. The minimum resolution measured by the gaussmeter probe is 0.01 Gauss with 1% accuracy. The gaussmeter probe with 4-digit readout provides accuracy of $\pm 1\%$ full scale and resolution of 0.05% full scale in three

ranges from 200 Gauss to 20 kilo Gauss full scale. A pickup coil, made of 30 turns of 33 AWG wire, is coiled around the rod sample; and its output was fed into a fluxmeter (Polytronic FM-110) to estimate the magnetic flux density. The fluxmeter (Polytronic FM-110) with 4-digit readout provides accuracy of $\pm 0.5\%$ full scale and is calibrated in Maxwell. Its minimum measuring resolution is 1 kMT (kilo maxwell Turns) and can measure up to 100000 kMT. We measure the magnetostriction with a strain gauge (LCT CF350-3AA) bonded along the longitudinal direction of the specimen, wired to a high-frequency dynamic strain data acquisition system (AG Measurematics AM-425) in a quarter bridge configuration. The measurement resolution of the strain data acquisition system is 1μ strain with an accuracy of 1% of the indicated strain value. The magneto-strain data are acquired from the ADSOF-H application software.

5.2.2. Magneto-elastic compression test

The same magnetic and mechanical operating regimes prevail in the actual design of the Terfenol-D-based transducers have been considered in this experiment as shown in **Figure 5.2.** The environment delineated is used to evaluate the compressive stress-strain curves of Terfenol-D under the regulated quasi-static circumstances. The nonlinear behaviour of stress-strain curves are obtained for the Terfenol-D rod samples of 8 mm diameter and 28 mm length in accordance with ASTM E9-19 (2019). Most Terfenol-D transducers have magnetic operating regimes ranging between 0.02 T to 0.05 T. Thus, a solenoid along with a DC power supply (GW INSTEK GPE 4323) is employed to generate magnetic fields up to 0.05 T. The Terfenol-D rod longitudinal strain is measured under the three different constant magnetic field levels (i.e., 0 T, 0.03 T and 0.05 T) using a strain gauge (LCT CF350-3AA) mounted directly under the solenoid in the centre of rod specimen using a dynamic strain data acquisition system (AM-425). One specimen in the absence of magnetic field and one specimen for each magnetic field (i.e., 0.03 T and 0.05 T) are tested up to 140 MPa at room

temperature using INSTRON UTM 3367. The specimens were prepared with the utmost care as per the laid down ASTM standard regarding the surface quality and planeness of the specimens within tolerance limits. A strain rate of 0.1 mm/min is maintained throughout the experimentation.

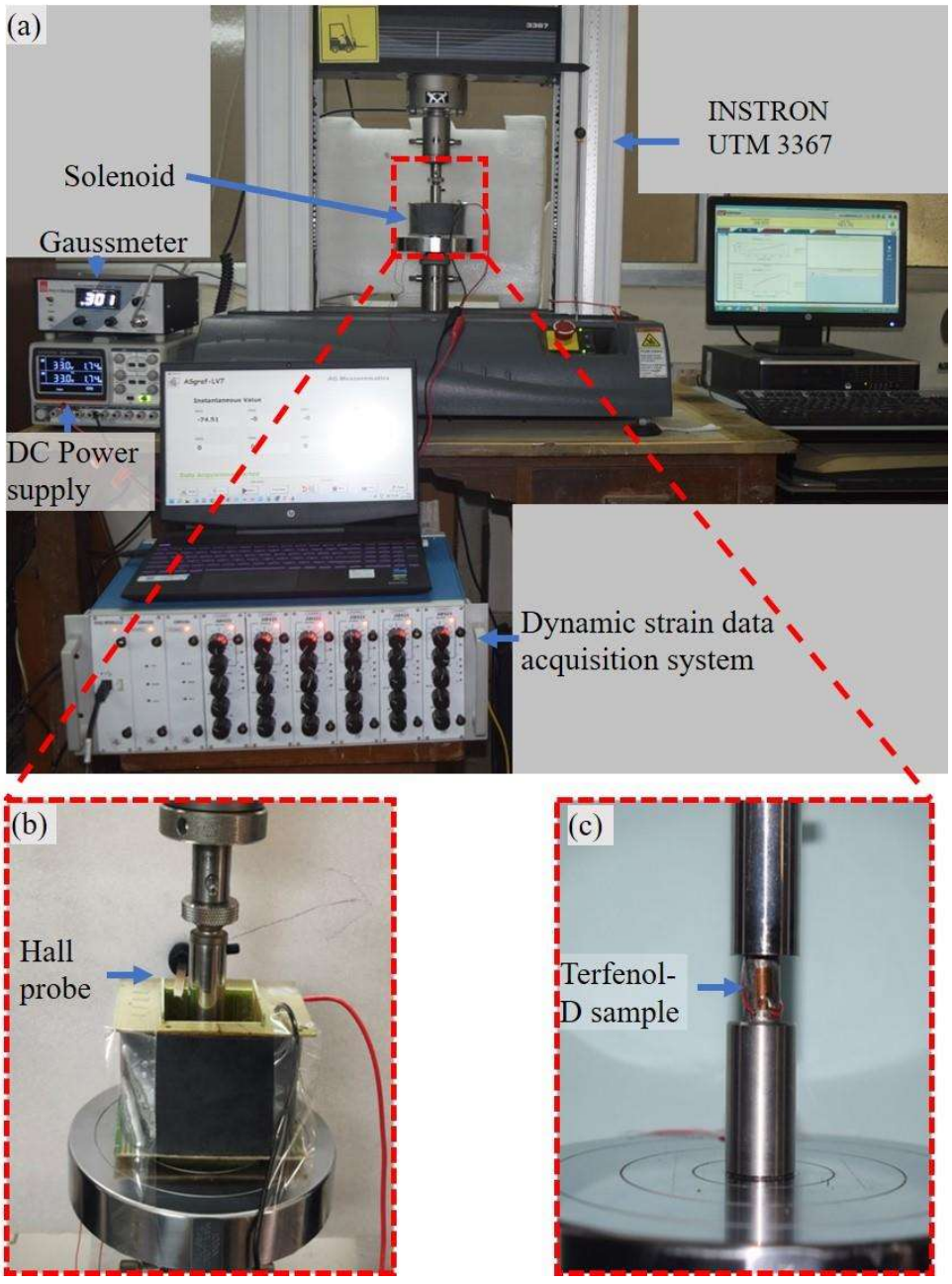

Figure 5.2: (a) Coupled field compression test setup **(b)** Zoomed view of Hall probe and solenoid **(c)** Arrangement of Terfenol-D rod specimen inside the solenoid in a zoomed-in perspective.

5.3. Numerical Analysis

The rotation of magnetic domains due to tensile and compressive pre-stresses causes nonlinear elastic strains in the giant magnetostrictive material. To account for this nonlinear characteristic, a novel vector function of the hyperbolic tangent was developed in Chapter 3 [127] based on the physical facts of magnetostrictive volumetric strain [4] and isotropic elasticity theory. Based on above functions, a three-dimensional magneto-elastic nonlinear anhysteretic constitutive relations are formulated in Chapter 3 for the isotropic and homogenous giant magnetostrictive materials. The hysteretic magnetic induction $\boldsymbol{B}$ and the nonlinear hysteretic magneto-strain can be evaluated using Eqs. (3.29), (3.30), (3.36), and (3.41), under the coupled influence of the applied magnetic field, prestresses. This section introduces a numerical framework similar to section 3.5 for evaluating the giant magnetostrictive material's response, governed by the coupled magneto-elastic physics. The presented constitutive relations in the preceding section are governed by the coupling of the Maxwell equation in the absence of volume charge and equilibrium equations for a stressed continuum of volume V subjected to arbitrary traction and body forces f_i. These coupled equations in tensor form can be written as

$$B_{i,j} = 0 \;\; and \;\; \epsilon_{ijk} H_{k,j} = 0 \tag{5.1}$$

$$\sigma_{ij,j} + f_i = \rho \ddot{u}_i \tag{5.2}$$

where, u_i is the displacements, ρ is the mass density and ϵ_{ijk} is the Levi-Civita symbol. A comma followed by an index denotes the partial differentiation with respect to the spatial coordinates x, y, z.

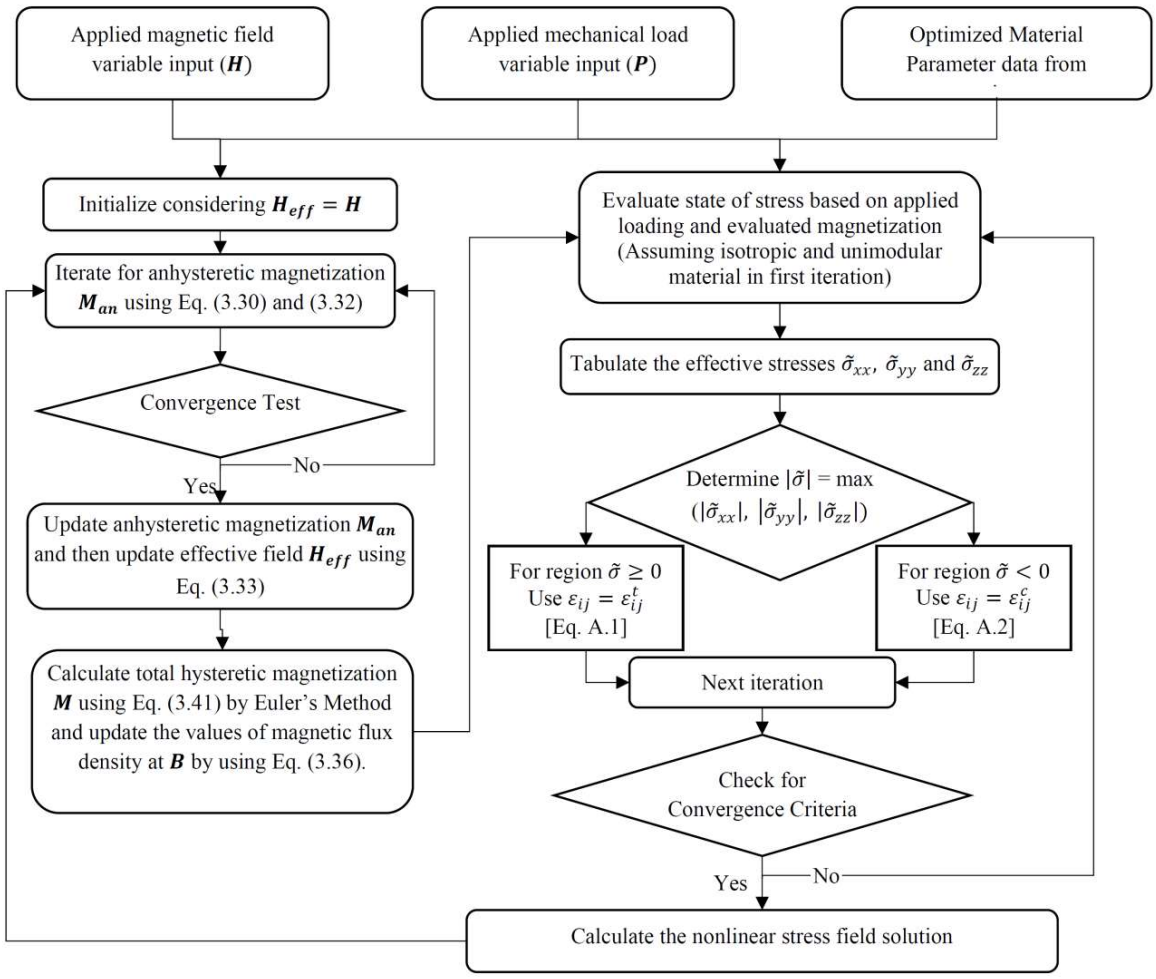

Figure 5.3 A solution algorithm for the coupled nonlinear hysteretic constitutive model for evaluating material's nonlinear responses

Due to the previously demonstrated nonlinear coupling, Equations (3.29) and (3.30) are nonlinearly reliant on the unknowns at each time step, through magnetization M, magnetostriction λ, nonlinear stress σ_{ij} and strain ε_{ij} when an applied field and loads are specified. An iterative strategy is presented in the flowchart as shown in **Figure 5.3** to solve this nonlinear coupling for estimating the Terfenol-D response variables. The main solution steps of the approach are briefly described here.

Step 1. Input the magneto-mechanical loading variables and the requisite material parameters optimized from physical and experimental evidence.

Step 2. At the initial time step $t = 0$, the first iteration is initiated by assuming the isotropic and unimodular material and the stress (σ_{ij}), strain (ε_{ij}) values can be predicted with the help of Eq. (3.29). Subsequently, the anhysteretic magnetization $\mathbf{M_{an}}$ can be computed iteratively with Eq. (3.31) [or Eq. (3.29)] and initialized under the assumption of $\boldsymbol{H_{eff}} = \mathbf{H}$.

Step 3. Determine the modified $\boldsymbol{H_{eff}}$ with the help of previously compute $\mathbf{M}_{an}^{prev}$. The modified $\boldsymbol{H_{eff}}$ is then used to predict the new revised value of $\mathbf{M_{an}}$. The iteration is repeated till the convergence criterion is satisfied $\left(\text{i. e.} \frac{|\mathbf{M_{an}} - \mathbf{M}_{an}^{prev}|}{|\mathbf{M}_{an}^{prev}|} < 0.001\right)$.

Step 4. Calculate the hysteretic magnetization $\mathbf{M}$ as expressed in Eq. (3.41) by applying the Euler's method with the aid of obtained values of $\mathbf{M_{an}}$ and $\boldsymbol{H_{eff}}$ and then hysteretic magnetic induction $\boldsymbol{B}$ is computed using Eq. (3.36).

Step 5. On the basis of evaluated stress-strain values in step 1, calculate the deviatoric effective stresses $\tilde{\sigma}_{xx}$, $\tilde{\sigma}_{yy}$ and $\tilde{\sigma}_{zz}$, and determine the $|\tilde{\sigma}|$ = max ($|\tilde{\sigma}_{xx}|$, $|\tilde{\sigma}_{yy}|$, $|\tilde{\sigma}_{zz}|$). Then the iteration invokes the conditional statement to identify the regions for $\tilde{\sigma} \geq 0$ or $\tilde{\sigma} < 0$, and subsequently, using the modified hysteretic magnetization $\mathbf{M}$ (calculated in step 4), assign the strain relation as $\varepsilon_{ij} = \varepsilon_{ij}^{t}$ [Eq. (A.1)] or $\varepsilon_{ij} = \varepsilon_{ij}^{c}$ [Eq. (A.2)], respectively [see Appendix A]. Since, Equations (3.29) and (3.30) are nonlinearly coupled, this solving progress is accomplished by the logical iteration loops until the convergence criterion based on the state of stress ($\|\boldsymbol{\sigma}\| < 0.001$) is met and the difference in stress state ($\|\boldsymbol{\sigma}\|$) between two consecutive iterations remains constant for 99.99% of the assigned nodes. Hence, the nonlinear stress field solution can be evaluated for the set of applied magneto-elastic loading variables.

Step 6. In the next time step $t + \Delta t$, updated values of the anhysteretic magnetization $\mathbf{M_{an}}$ can be computed iteratively by applying the nonlinear stress field solutions using Eq. (3.32).

This loop is executed repeatedly until the last time step, at which point the materials response to the desired coupled field variable loading is evaluated.

5.3.1. Solution method in COMSOL

The magnetic field-no currents and solid mechanics modules in coupling with domain ODEs module of the finite-element based tool COMSOL Multiphysics are used to solve this coupled physics event numerically as shown in **Figure 5.4**. The multiphysics environment includes meshing tool, local to global matrix assembly, postprocessing and visualization toolbox for efficient analysis. The finite element procedure involves solution domain partitioning while allowing different subdomains to have varying degrees of freedom.

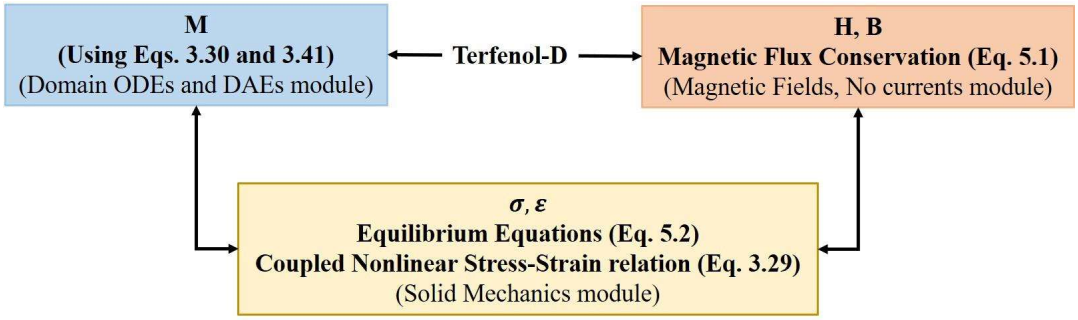

Figure 5.4: Schematic diagram of multiphysics calculation module for coupled magneto-elastic response of Terfenol-D

The magnetic field-no currents module in COMSOL provides us with surrounding magnetic field and take into account the magnetic properties. The directional magnetic field is applied on the boundaries of air domain. For Terfenol-D, the magnetization is nonlinear and stress dependent, thus we need to model the magnetic hysteresis response as presented in the Eq. (3.41) [or in Eq. (3.30)] in the external material node using the general $\boldsymbol{H}(\boldsymbol{M})$ relation. Due to the magneto-elastic response i.e., strain and effective magnetic field of Terfenol-D is coupled and depends on stress (see Eq. (3.29) and Eq. (3.41)) an infinite loop will appear if they are computed directly by software. Thus, an ODEs module is adopted, and iterative method is used to calculate Eq. (3.41) and value of $\boldsymbol{M}$ is inputted to the magnetic field-no

currents module. For a particular state of a magnetic field, the magnetic flux density and magnetic scalar potential are governed by the Maxwell equations as presented in Eqs. (5.1) and (5.2), and the magnetic flux density distribution in both materials is calculated using Eq. (3.36).

Then the solid mechanics module is used to evaluate the nonlinear stress-strain state of the magnetostrictive material. The stress and magnetization dependent nonlinear stress-strain relation proposed in Eq. (3.29) can be implemented as the external material function or by superimposing the magnetostrictive pre-strain on the linear elastic model. For a specified loading conditions, the equilibrium of the nonlinear stress field is governed by the Eqs. (5.1)-(5.2) and the nonlinear stress field is evaluated iteratively until the convergence criterion $\|\boldsymbol{\sigma}\| < 0.001$ is satisfied. The stress-strain and general $\boldsymbol{H}(\boldsymbol{M})$ relation is written in C programming language using Eq. (3.29) and Eq. (3.41). The C program code is then compiled into a shared library that COMSOL Multiphysics can access at runtime. Hence, by following the aforementioned scheme, the Terfenol-D responses can be evaluated for a variety of initial and boundary circumstances.

5.3.2. Numerical model for magneto-elastic response of material

In the numerical analysis, a pre-stressed Terfenol-D rod placed in the uniformly applied magnetic field is modelled using the 2-D axisymmetric space for the transient analysis. **Figure 5.5** depicts the mapped meshing of Terfenol-D rod and triangular meshing of air domain surrounding the rod for high quality simulations. It is worth noting that the magnetic flux density distribution adheres to the homogeneous value of 1 T when the external applied magnetic field is 0.5 T.

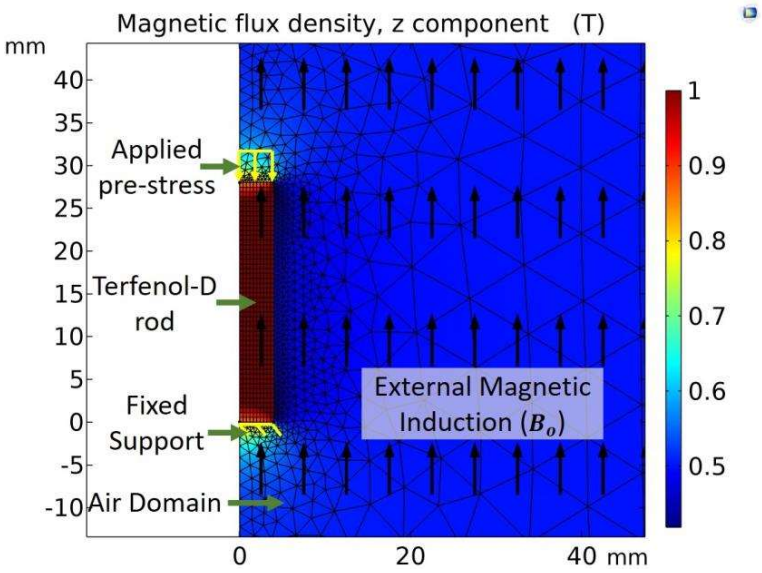

Figure 5.5: Mapped meshing and magnetic flux density distribution along the longitudinal direction of Terfenol-D rod in the 2D axisymmetric space

5.4. Results and Discussions

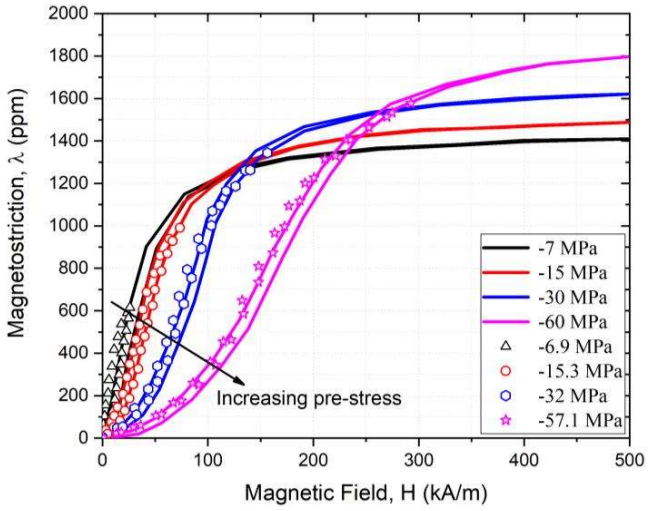

Figure 5.6 Comparison of magnetostriction curves obtained by the present experiment with the Moffett et al.'s [14] experiment at different pre-stress levels

In this section, we first compare the experimental data of the magnetostriction curves performed by Moffett et al. [14] with the experimental data obtained in present work (see **Figure 5.6**) to verify the reliability and repeatability of the present experimentation system. **Figure 5.6** demonstrates that our results closely resemble those of Moffett et al. [14]. Then,

we will compare the experimental response of the giant magnetostrictive material (i.e., Terfenol-D) against the coupled constitutive predictions for validation. Based on the physical and experimental evidence for magnetization and magnetostriction curves, the material properties are calibrated for the Terfenol-D specimens. The material parameters are optimized to be further used in the constitutive model of the numerical analysis. Then, experimental and simulation analyses of uniaxial compression were carried out on Terfenol-D samples in both presence and absence of an externally applied magnetic field. The purpose of this exercise is to reaffirm the constitutive relations validity in the high stress regions and to verify the capabilities of the suggested finite element based numerical approach.

5.4.1. Comparison between hysteretic magnetic response experiments and simulation

A comparison of coupled magneto-elastic experiments and simulations were performed to calibrate the parameters of the hysteretic magneto-elastic constitutive relations. Since the thin rod specimen is placed in contact with soft iron pole pieces, the geometric demagnetization losses will be negligible along its longitudinal axis [56] and the value of demagnetizing factor can be taken as $N = 0$. **Figure 5.7** highlights the experimental and simulation data for the magnetization and magnetostriction curves under the applied magnetic field at different pre-stress levels. Then calibrated material properties are evaluated for the Terfenol-D and listed in Table 5-1. The same are subsequently used in the numerical computations. The magnetization and magnetostriction curves of a giant magnetostrictive material exhibit saturation phenomenon and are sensitive to applied prestresses and the magnetic field. The comparisons reveal that the magnetization and magnetostriction curves generated by numerical simulation (solid lines) are in good agreement with those reported by the experiments (dashed lines) at various pre-stress levels in all regions of applied field. The average root mean square error remains around 1.08% and that explains the capability and reliability of magneto-elastic coupled hysteresis constitutive model.

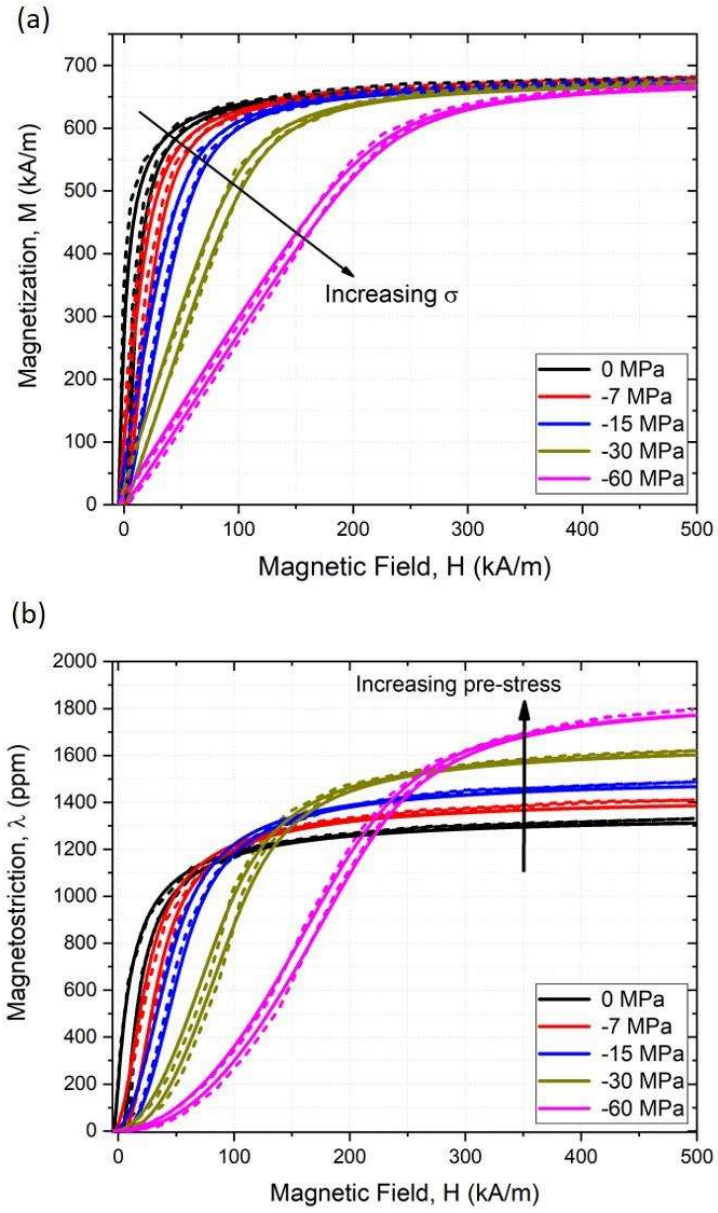

Figure 5.7 Comparison of the Magnetization and Magnetostriction hysteresis curves predicted by the constitutive model under various pre-stress levels with experimental results at room temperature. (Dashed lines: experimental curves; solid lines: theoretical predictions)

Table 5-1 Material properties of the Terfenol-D specimens

Property	**Terfenol-D**
M_s $(\times 10^5\ \mathrm{A/m})$	6.8
λ_s (ppm)	1350
σ_s (MPa)	120
E_{in}(GPa)	90
η'	0.04
c	0.1
χ_m	31
K (A/m)	6000
ν	0.25

5.4.2. Comparison between compression experiment and simulation

The poor tensile strength [18] and high brittleness of Terfenol-D makes it susceptible to in-service fracture. Singularity of the stress field at the notch tip results in high stress gradient zones in the fracture specimen. So, for the fracture characterization of Terfenol-D, it is critical to compare the nonlinear experimental stress-strain curves with the numerical ones, particularly in the region of high pre-stresses. From **Figure 5.8 (a)**, it is observed that the stress-strain hysteresis curves calculated by the numerical model exhibit an explicit agreement with the experimental data for the considered three different magnetic field levels (i.e., 0 T, 0.03 T and 0.05 T). It is evident from the Young's modulus vs compressive stress curves (**Figure 5.8 (b)** that the numerical model is precisely able to predict the ΔE effect. At 0 T (No magnetic field), it is seen that with the increase in compressive stress, the Young's modulus curve rises asymptotically towards the saturated intrinsic Young's modulus value, whereas, in the presence of magnetic field (0.03 T and 0.05 T), the value of Young's modulus initially decreases from its zero-stress value to attain a minimum and then approaches to intrinsic values. This explains the significance of combined effect of magnetic field with a

mechanical loading environment influencing the elastic modulus and hence stiffness characteristics of component in design.

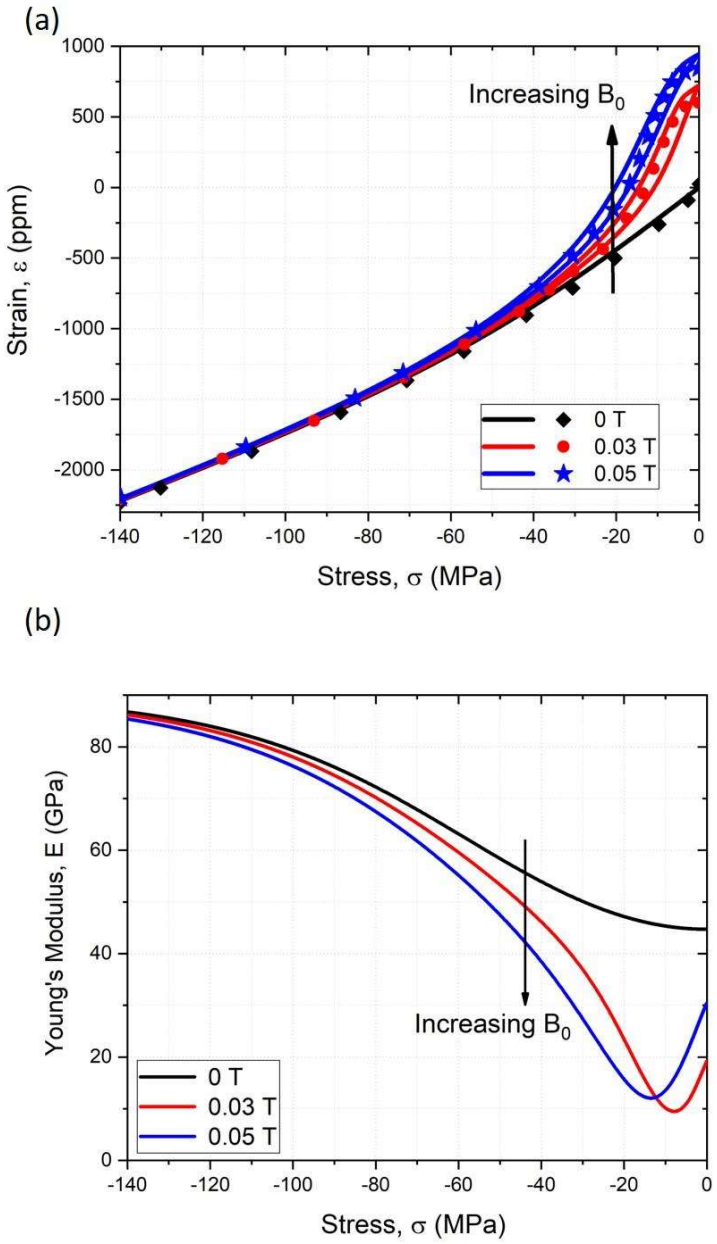

Figure 5.8 (a) Comparison of compressive strain vs compressive stress curves predicted by the constitutive model with the experimental results at room temperature (Scatters: experimental curves; solid lines: theoretical predictions) **(b)** Young's modulus vs compressive stress curves

5.5. Summary

In this chapter, an appropriate experimental and numerical analysis is conducted to determine the magnetostrictive material properties needed to use in the proposed constitutive model for numerical fracture characterization. Physics-based experiments has been conducted to characterize hysteretic magnetic response for stress-strain, magnetization and magnetostriction loops. Terfenol-D magnetization and magnetostrictive properties are sensitive to magnetic and mechanical bias conditions; therefore, a precise finite element based model has been created. Then numerical analysis is performed to calibrate the material parameters for the proposed constitutive model consistent with the experimental hysteretic magnetic response curves.